Pergamon

Bioorganic & Medicinal Chemistry 7 (1999) 1309–1319

BIOORGANIC & MEDICINAL CHEMISTRY

Exploring the Conformation of Bilirubins with Natural and Unnatural Analogues: Use of Positional and Bridged Isomers of Bilirubin IXα

Marcelo J. Kogan,[a] María E. Mora,[b] Sara E. Bari,[b] José Iturraspe,[a] Josefina Awruch[b] and José M. Delfino[a,*]

[a]*Departamento de Química Biológica, Facultad de Farmacia y Bioquímica, Universidad de Buenos Aires, Junín 956, 1113 Buenos Aires, Argentina*

[b]*Departamento de Química Orgánica, Facultad de Farmacia y Bioquímica, Universidad de Buenos Aires, Junín 956, 1113 Buenos Aires, Argentina*

Received 17 August 1998; accepted 2 December 1998

Abstract—Unlike bilirubin IXα (**1**), the isomers bilirubin IXδ (**2**) and neobilirubin IXβ (**3**) do not require conjugation with glucuronic acid in order to be excreted. A conformational analysis employing an optimized Monte Carlo method and a mixed Monte Carlo/stochastic dynamics reveals that isomer **2** exhibits a structure more closed than the well known 'ridge-tile' conformation of **1**. The change in the position of both propionic acid chains causes the loss of at least four hydrogen bonds. On the other hand, the change in the configuration of the distal dipyrrinone and the blockage of the lactamic nitrogen by the presence of a bridge in isomer **3** results in an open and more elongated structure, where the chance of hydrogen bond formation in this region is obliterated. The resulting molecular models for these compounds are consistent with ^{1}H NMR, UV–vis, and TLC data.

Introduction

Most natural bile pigments exhibit the configuration of the IXα isomer because the cleavage of the cyclic heme molecule is a regioselective reaction occurring preferably at the α-*meso*-bridge carbon.[1–3] In most mammals, heme is converted at the α-methene bridge into biliverdin IXα by heme oxygenase, and this product is in turn reduced to bilirubin IXα by the cytosolic enzyme biliverdin reductase. The latter pigment is excreted into the bile after conjugation, a reaction catalyzed by UDP-glucuronosyltransferase.[4–6] Small amounts of isomers of bilirubin IXα have been found under both physiological and pathological conditions in vivo[6–9] or in isolated perfused rat liver.[10]

Unlike isomer IXα, bilirubins IXβ, IXγ and IXδ were excreted in bile without conjugation. Thence it was proposed that these bilirubins adopt conformations which confer them polar properties, thus allowing their excretion into bile as their unconjugated forms.[11,12] Besides, intramolecular hydrogen bonds between propionic carboxylates and lactamic and pyrrolic NHs of bilirubin IXα seem to be important for bilirubin conjugation.[13] In this regard, we demonstrated that increasing the hydrophilicity of bilirubin by substitution with extra propionic acid chains leads to the excretion of the unconjugated pigment, even when this compound is able to form intramolecular hydrogen bonds similar to those found in bilirubin IXα.[14] Recently, we studied two monopropionic analogues—both more hydrophilic than bilirubin IXα—and found that the compound substituted with a propionic acid chain in C_8 is excreted in bile conjugated with glucuronic acid, whereas a positional isomer similarly substituted at C_7 is excreted without conjugation. A conformational analysis of these two analogues revealed that the former adopts a 'ridge tile' conformation, stabilized by the presence of three intramolecular hydrogen bonds, whereas in the latter compound impairment in the formation of at least one hydrogen bond occurs.[15]

For this study we chose a positional and a bridged isomer of bilirubin IXα (**1**), namely, bilirubin IXδ (**2**) and neobilirubin IXβ (**3**), appropriate for probing structural features relevant for glucuronidation. The hepatobiliary excretion of these two isomers was investigated through the use of their corresponding synthetic biliverdin

Key words: Bilirubin isomers; glucuronidation; conformational search; Monte Carlo; stochastic/molecular dynamics; hydrogen bonds.
* Corresponding author. Tel.: (5411) 4962 5506 and (5411) 4964 8291; fax: (5411) 4962 5457; e-mail: rtdelfin@criba.edu.ar

0968-0896/99/$ - see front matter
PII: S0968-0896(99)00067-X

precursors, based on the fact that biliverdins bearing two propionic acid chains are substrates in vitro of biliverdin reductase.[16,17] Molecular mechanics simulations shed light on the preferred conformations of these isomers. In particular, we focused our analysis on the importance of the intramolecular hydrogen bond network for determining the overall properties of these compounds. Results from our theoretical calculations are discussed in connection with experimental data of the in vivo excretion of these pigments, measurements of their polarity by TLC, and ^{1}H NMR and UV–vis spectroscopical evidence.

Results

Choice of positional and bridged isomers of bilirubin IXα as targets for this study

We chose to study a linear (**2**) and a bridged (**3**) isomer of bilirubin IXα (**1**) endowed with propionic acid chains on C_3 and C_7 (Schemes 1 and 2). The current view[13,15] holds that substitution at C_8 and C_{12} would lead to the formation of six hydrogen bonds, whereas the propionic acid chain attached to C_3 or C_7 would fail to establish at least some of these intramolecular hydrogen bonds. In addition, the expectation is that the change in configuration of the distal dipyrrinone (rings C and D) and the blockage of the lactamic nitrogen by the presence of an ethylene bridge between N_{24} and C_{13} in isomer **3** would further reduce the chance of hydrogen bond formation.

The parent biliverdins **4** and **5** (Scheme 1) employed in studies in vivo were synthesized as follows. The dimethyl ester **6** was obtained from protohemin IX using the coupled oxidation method.[18] Saponification of the diester to yield **4** was performed as described elsewhere.[19] Structure determination of the diacid was established as described.[20,21] The dimethyl ester **7** was prepared by total synthesis[22] and the product was saponified to the acid **5** as described below (see Experimental).

Physicochemical and spectroscopic properties of isomers of bilirubin IXα

Bilirubin **2** (R_f 0.74) and bilirubin **3** (R_f 0.70) exhibit similar polarity and both are more polar than unconjugated bilirubin **1** (R_f 1). The UV–visible spectrum in methanol or chloroform of compound **2** shows a band with an absorption maximum at 394 nm. At variance with this, the spectrum of bilirubin **3** is red-shifted (maximum at 433 nm).

^{1}H NMR spectra (taken in deuterated chloroform) of these isomers of bilirubin IXα reveal the extent of hydrogen bonding. The presence or absence of hydrogen bonds can be monitored by the position of signals corresponding to the NHs or the carboxyl OHs. The analysis of these spectra focused on the chemical shifts

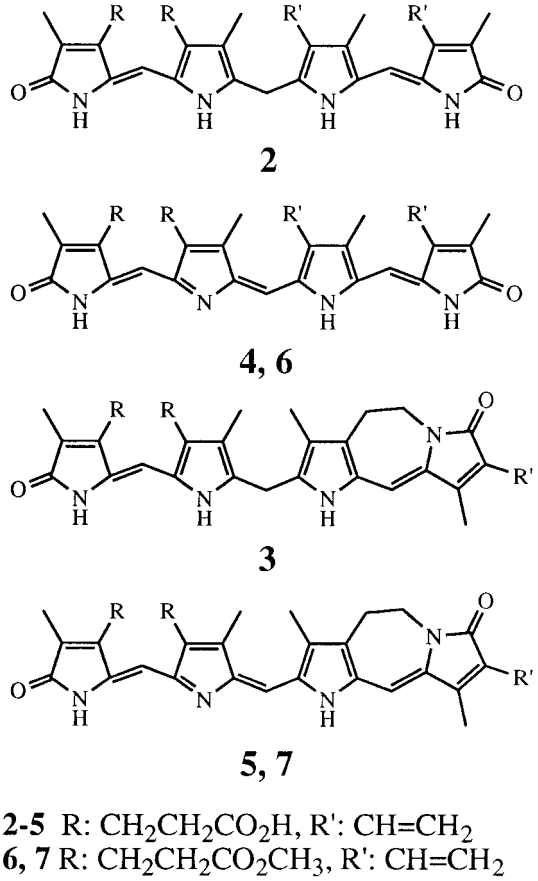

Scheme 1.

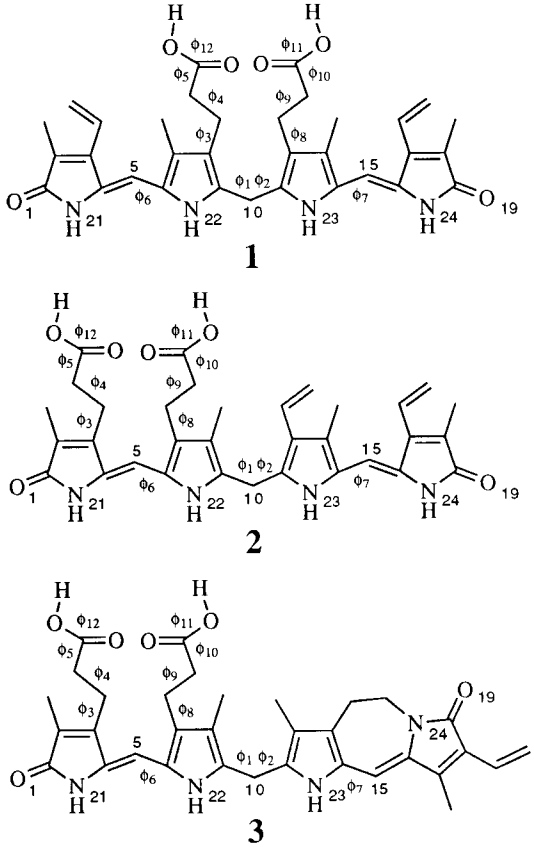

Scheme 2.

of these signals, after the chemical class of each proton had been ascertained by H/D exchange experiments. Compound **2** exhibits the following signals: 14.35 and 13.24 ppm for the acidic OHs, 10.62 and 10.19 ppm for the pyrrolic NHs, and 9.35 and 9.21 for the lactamic NHs. Collection of ^{1}H NMR data on compound **3** was hindered by the rapid oxidation of this a,c-biladiene to the corresponding a,b,c-bilatriene in the process.

Biological assays in vivo

Because of the high susceptibility to oxidation shown by bilirubin **3** during manipulation, the metabolism of both bilirubins tested in this paper was studied starting from the corresponding biliverdins. Compounds **4** and **5** were shown to be efficiently metabolized into bilirubins **2** and **3** (Fig. 1, panels c and d versus panels a and b, respectively). In order to test if the latter are excreted in bile fluid as such or rather as their glucuronides, the corresponding biliverdins were injected in the bloodstream of male Wistar rats. The analysis by TLC of bilirubin components present in this fluid showed that both bilirubins were excreted in bile entirely as their unconjugated forms. The competence of the hepatobiliary glucuronidation machinery under the conditions of this assay was ascertained by the normal level of excretion of the conjugates of endogenous bilirubin **1**.

A similar time course was observed for the excretion of both bilirubins. The concentration in bile of both unconjugated forms reached a maximum before 30 min after injection and insignificant levels of any of these compounds were seen after 90 min. However, compound **3** appears to be cleared from bile somewhat more rapidly than compound **2**.

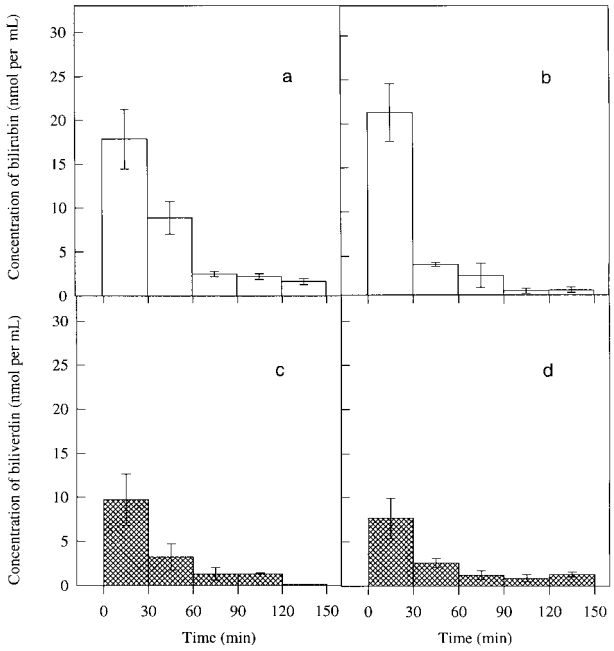

Figure 1. 'In vivo' excretion of bilirubin isomers in rat bile. The time course of excretion of isomers **2** and **3** is shown in panels a and b, respectively. The concentration of the parent biliverdins **4** and **5** is shown below in panels c and d, respectively. Data for each analogue assayed are expressed as the mean value ± standard error of four independent experiments. Bile (0.35 ± 0.05 mL) was collected at each time point. The concentration (nmol/mL) of endogenous free bilirubin IXα (**1**), its monoglucuronide and its diglucuronide ranged between the limits shown below: (a and c) 1–2, 19–27, 10–22; and (b and d) 0.8–1, 18–28, 7–10. For details see Experimental.

Conformational analysis

Optimized Monte Carlo search, energy minimization and relative stability of isomers. Molecular models for compounds **1–3** were initially constructed using the model-building facility implemented in MacroModel.[23] Coordinates for these structures were used as input for BatchMin, the calculation module of this program.

In order to search the conformational space available to these compounds, we ran an optimized Monte Carlo protocol which allowed free rotation around all dihedral angles (Φ_i, as indicated in Scheme 2). These torsions constitute the major determinants of the structure. Planar structures were chosen as starting geometries for bilirubins **1–3**, i.e. the Φ_1,Φ_2 central pair of torsion angles adopted the following values: 0,180; 180,0; 0,0 and 180,180°. Dihedral angles along the propionic acid chains were set to an all anti conformation and the remainder were as shown in Scheme 2. For compound **3** the unsaturated azepine ring was set to a half chair conformation. After this calculation, structures corresponding to the energy minima (as calculated with the force field MM2*) falling within a 5 kcal/mol window above the global minimum are shown in Table 1. In all cases, regardless of the choice of the initial structure, this search yielded the same set of conformers.

In order to calculate the heats of formation of these compounds, the minimized structures were used as input for the semiempirical method AM1, as implemented in HyperChem.[24] After convergence is reached, a single point calculation was run to yield these values (Table 1).

Within this energy window, a unique structure was found for bilirubin IXα. This conformer (**1**, Table 1) did not differ significantly from that found by others[13] or from the crystallographic structure.[25,26] This compound adopts a typical 'ridge tile' conformation, stabilized by the presence of six hydrogen bonds forming between each dipyrrinone system and the propionic side chain located on the opposite half of the molecule.

On the other hand, bilirubin IXδ (**2**) yielded three distinct non-enantiomeric conformers. The global minimum structure of this compound (**2$_1$**) adopts a somewhat more closed conformation than that found for **1**. Structure **2$_1$** shows the presence of two hydrogen bonds between the propionic acid chain at C_7 and the opposite dipyrrinone. The nonbonded distances ($CO_7{}^3\ldots H_{23}N$ and $OH_7{}^5\ldots O_{19}C$) fall within acceptable limits for hydrogen bonding. Conversely, distance ($CO_7{}^3\ldots H_{24}N$) exceeds the limit for an average hydrogen bond (2.76 Å). Likewise, it can be seen that the dihedral angles determining the conformation of the propionic acid side chain at C_7 in this conformer, (i.e.

Table 1. Conformations corresponding to energy minima for compounds **1**, **2** and **3**[a]

Conformer[a]	**1**		$\mathbf{2_1}$	$\mathbf{2_2}$	$\mathbf{2_3}$	$\mathbf{3_1}$	$\mathbf{3_2}$	$\mathbf{3_3}$
Dihedral angle (°)[b]								
Φ_1	−57		−39	101	−83	34	18	−112
Φ_2	−57		−53	−21	−10	60	−108	−114
Φ_3	−120		−93	98	−98	98	97	−81
Φ_4	62		51	−61	70	−59	−61	82
Φ_5	1		−90	−54	−13	80	81	82
Φ_6	−9		33	32	−28	−35	−35	−28
Φ_7	−10		28	−40	33	175	171	170
Φ_8	−120		99	−97	95	−90	−90	98
Φ_9	62		−51	47	−41	82	82	−68
Φ_{10}	1		78	−83	78	85	84	83
Distance (Å)[b]		Distance (Å)[b]						
$CO_8^3 \ldots H_{23}N$	1.755	$CO_7^3 \ldots H_{23}N$	2.765	1.930	1.908	> 3.0	> 3.0	> 3.0
$CO_8^3 \ldots H_{24}N$	1.753	$CO_7^3 \ldots H_{24}N$	1.873	2.984	1.951			
$OH_8^5 \ldots O_{19}C$	1.708	$OH_7^5 \ldots O_{19}C$	1.725	> 3.0	1.899	> 3.0	> 3.0	> 3.0
$CO_{12}^3 \ldots H_{22}N$	1.755	$CO_3^3 \ldots H_{23}N$	> 3.0	> 3.0	> 3.0	> 3.0	> 3.0	> 3.0
$CO_{12}^3 \ldots H_{21}N$	1.750	$CO_3^3 \ldots H_{24}N$	> 3.0	> 3.0	> 3.0			
$OH_{12}^5 \ldots O_1C$	1.711	$OH_3^5 \ldots O_{19}C$	> 3.0	1.696	1.725	> 3.0	> 3.0	> 3.0
$CO_8^3 \ldots H_{12}^5O$	> 3.0	$CO_3^3 \ldots H_7^5O$	2.097	1.720	1.847	1.746	1.746	1.720
$CO_{12}^3 \ldots H_8^5O$	> 3.0	$CO_7^3 \ldots H_3^5O$	1.963	> 3.0	> 3.0	1.717	1.711	1.753
Energy[c] (kcal/mol)	0.00		0.00	0.19	0.32	0.00	0.19	2.08
H_f[c] (kcal/mol)	−120.50		−108.07	−108.70	−108.30	−122.30	−122.50	−119.50

[a]All minima within a 5 kcal/mol window above the global minimum are reported here. After visual inspection of each structure, only non-superimposable and non-enantiomeric conformers are described.
[b]The definition of dihedral angles follows the convention: Φ_1: $N_{22}C_9C_{10}C_{11}$; Φ_2: $N_{23}C_{11}C_{10}C_9$; Φ_3: $C_9C_8C_8{}^1C_8{}^2$ (**1**) or $C_4C_3C_3{}^1C_3{}^2$ (**2**, **3**); Φ_4: $C_8C_8{}^1C_8{}^2C_8{}^3$ (**1**) or $C_3C_3{}^1C_3{}^2C_3{}^3$ (**2**, **3**); Φ_5: $C_8{}^1C_8{}^2C_8{}^3O_8{}^3$ (**1**) or $C_3{}^1C_3{}^2C_3{}^3O_3{}^3$ (**2**, **3**); Φ_6: $N_{22}C_6C_5C_4$; Φ_7: $N_{23}C_{14}C_{15}C_{16}$; Φ_8: $C_{11}C_{12}C_{12}{}^1C_{12}{}^2$ (**1**) or $C_6C_7C_7{}^1C_7{}^2$ (**2**, **3**); Φ_9: $C_{12}C_{12}{}^1C_{12}{}^2C_{12}{}^3$ (**1**) or $C_7C_7{}^1C_7{}^2C_7{}^3$ (**2**, **3**); Φ_{10}: $C_{12}{}^1C_{12}{}^2C_{12}{}^3O_{12}{}^3$ (**1**) or $C_7{}^1C_7{}^2C_7{}^3O_7{}^3$ (**2**, **3**); Φ_{11}: $C_{12}{}^2C_{12}{}^3O_{12}{}^4H_{12}{}^5$ (**1**) or $C_7{}^2C_7{}^3O_7{}^4H_7{}^5$ (**2**, **3**); Φ_{12}: $C_8{}^2C_8{}^3O_8{}^4H_8{}^5$ (**1**) or $C_3{}^2C_3{}^3O_3{}^4H_3{}^5$ (**2**, **3**) (see Scheme 2). Torsions Φ_{11} and Φ_{12} were held fixed at 180°. Values represent dihedral angles and bond distances obtained after the MC optimized method[40] employing the MM2* force field.
[c]Energy values calculated after molecular mechanics (MM2*) are reported as differences with respect to the global minimum. Heats of formation (H_f) calculated with AM1 are shown below.

Φ_8 and Φ_9) do not diverge much from the ideally expected values. Conspicuously, Φ_9 imposes a gauche conformation to the aliphatic chain, causing the end of the propionic side chain to orient in the general direction of the opposite dipyrrinone, thus allowing the formation of the above mentioned hydrogen bonds. Two other conformers ($\mathbf{2_2}$ and $\mathbf{2_3}$) were also observed. At variance with $\mathbf{2_1}$, these structures show the propionic acid chains at C_3 and C_7 involved in hydrogen bonding to the distal pyrrinone carbonyl group and pyrrolic NH, respectively.

The heats of formation of all conformers of **2** fall within a narrow limit and are about 12 kcal/mol higher than the value calculated for bilirubin IXα (**1**). In spite of the appearance of COOH/COOH hydrogen bonds in conformers **2**, this difference in energy can be accounted for by the loss of between 3–4 stable COOH/NH hydrogen bonds,[27] as arises readily by comparison between the global minimum structures $\mathbf{2_1}$ and **1**.

On the other hand, the conformational search of isomer **3** produced three non-enantiomeric conformers, whose torsion angles are also shown in Table 1. None of these structures shows hydrogen bonds between either carboxylate and the opposite pyrrolic NH or the lactamic carbonyl. The two propionic acid substituents bridge between themselves through two hydrogen bonds. The lower values calculated for the heats of formation of these conformers, as compared to **2**, were attributed mainly to the presence of the intramolecular covalent bridge. In order to elaborate this point further, we ran a test calculation on two isomeric pyrromethenones, namely, a bridged *trans*-isomer identical to the right half of compound **3**, and a *cis*-isomer endowed with a vinyl substituent in place of the bridge. The former was about 12 kcal/mol more stable than the latter (results not shown). In addition, shuffling of side chains to fit the substitution pattern of compound **2** adds about 2 kcal/mol to the stabilization energy of compound **3**. Taken together, these factors account approximately for the calculated difference in heats of formation (approx. 14 kcal/mol), thus minimizing the role of other contributions, such as COOH/COOH hydrogen bonding, to the extra stability found for compound **3**.

An independent conformational search employing the AMBER* force field instead of MM2* produced the same set of minimum energy conformers for both isomers. In all cases, rigid body superimposition of the structures calculated with each force field resulted in RMS deviations of less than 0.6 Å. In addition, minimization of this set in the presence of chloroform yielded the same collection of conformers.

Mixed Monte Carlo/stochastic dynamics

The aim of this study was to generate a conformational ensemble from which to derive the average structure for each bilirubin isomer and, in particular, to appraise

more realistically the extent of intramolecular hydrogen bonding. We believe that results derived from this simulation provide an improved correlation with molecular properties, enhancing the picture obtained after MC and energy minimization. Towards this end, we applied a recently developed MC/SD method,[28] which we recently used with profit on monopropionic analogues of bilirubins.[15]

As pointed out before, the key determinants of the conformation of these molecules are the Φ_i dihedral angles described in Scheme 2. In the course of this simulation, free rotation was allowed around all these torsions. Several runs following the protocol described below were carried out starting from: (i) 'extended' structures ($\Phi_1,\Phi_2 = 180, 180°$), (ii) 'porphyrin-like' structures ($\Phi_1,\Phi_2 = 0, 0°$) or (iii) combined structures ($\Phi_1,\Phi_2 = 0, 180°$ or $180, 0°$). In all cases, average values for hydrogen bond distances and angles calculated on the final conformational ensemble were the same (results not shown).

After an initial equilibration period of 50 ps, each simulation was allowed to proceed for 6,000 ps at 300 K and produced as output a population of 400,000 conformers. This protocol ensures that the following convergence criteria are met: (i) the final average values for bond distances and bond angles are the same, regardless of the choice of starting structure; (ii) mean temperature and mean enthalpy reach numerical stability; and (iii) a symmetrical distribution for all freely rotating dihedral angles is observed. In all cases, the MC acceptance ratio[28] was never lower than 0.3% or higher than 5%. Further reassurance that convergence has indeed been reached was provided by the application of a novel MC method (jumping between wells: JBW algorithm)[29] developed to preferentially sample significantly populated regions in the energy landscape.

The most frequent values of Φ_i found along the MC/SD run are reported in Table 2, giving rise to the average structures represented in Figure 2. The sturdiness of the conformation of bilirubin IXα (**1**) is demonstrated by the persistence of all six hydrogen bonds along the MC/SD simulation. Consistent with this result, small deviations were found from the average values for torsion angles and hydrogen bond distances (see also Table 3). Compound **2** adopts a closely folded structure, more akin to the preferred conformation found for a monopropionic analogue of bilirubin substituted at C_7 (compound **6**, ref 15) than to the typical 'ridge-tile' conformation adopted by bilirubin IXα (**1**). The distances between the centroids of the pyrrinone rings measured for each average structure are reported in the legend to Figure 2. On the other hand, compound **3** exhibits an extended conformation where the ϕ_1,ϕ_2 torsion pair is not dissimilar from the values found for high energy local minima of bilirubin IXα ($\phi_1 = \phi_2 \approx 110°$, ref 13) or a monopropionic analogue substituted at C_8 (conformer $\mathbf{5_3}$, $\phi_1 = \phi_2 \approx -115°$, ref 15).

For compound **2**, the overall average conformation resembles more that found for conformer $\mathbf{2_3}$ (RMS deviation less than 0.30 Å) than that found for the global minimum (conformer $\mathbf{2_1}$ RMS≈1.37 Å). This is not surprising given the negligible energy difference that exists between these conformers. Moreover, and consistent with these facts, a close agreement was observed between the average conformation of compound **2** and the structure of minimum energy found in chloroform when employing the AMBER* force field (RMS deviation less than 0.25 Å, result not shown). Remarkably, large excursions are allowed for this compound, as evidenced by the wide spread of the distribution of torsion angles, in particular, for the critical pair Φ_1, Φ_2, cf. these values and distribution ranges found for compound **1**. Similarly, in the conformational ensemble of compound **3**, where extended forms predominate, a wide range of values for dihedral angles critical for the overall conformation was also observed.

The evidence presented in Table 3 indicates that compound **2** is able to form the $OH_7{}^3\ldots O_{19}C$ hydrogen bond in chloroform at 300 K. Comparatively, the $OH_3{}^5\ldots O_{19}C$ hydrogen bond is rarely observed. By contrast, an impairment exists for the establishment of the $CO_7{}^3\ldots H_{23}N$ and $CO_7{}^3\ldots H_{24}N$ bonds, the largest effect being observed for the former. A similar situation

Table 2. Most frequent dihedral angles for bilirubin IXα and its isomers encountered along the MC/SD simulation[a]

Conformer dihedral angle (°)[b]	Compound **1**	Compound **2**	Compound **3**
Φ_1	−60 (−50, −70)	−85 (−110, −55)	−105 (−75, −125)
Φ_2	−60 (−50, −70)	5 (−45, 40)	−110 (−130, −85)
Φ_3	−120 (−110, −130)	−95 (−70, −115)	95 (80, 110)
Φ_4	60 (40, 80)	60 (40, 80)	60 (40, 80)
Φ_5	0 (30, −30)	90 (60, 120)	−90 (−110, −70)
Φ_6	0 (20, −20)	20 (0, 40)	−20 (−40, 0)
Φ_7	0 (20, −20)	30 (15, 45)	170 (168, 174)[c]
Φ_8	−120 (−110, −130)	110 (100, 120)	100 (85, 110)
Φ_9	60 (70, 80)	−50 (−60, −40)	−65 (−80, −45)
Φ_{10}	0 (20, −20)	90 (70, 110)	95 (90, 110)

[a]MC/SD simulations at 300 K in chloroform employing the AMBER* force field were run for 6 ns. This time allows the calculation to converge according to the criteria mentioned in Experimental. Four hundred thousand conformers were sampled for each isomer.
[b]The definition of dihedral angles follows the convention described in the legend to Table 1. The values represent bond angles for the most populated states (mode), the limits for the width of the distribution bell at half height are reported between parentheses. For all angles, no other value was observed to be significantly populated.
[c]In this case, free rotation was disallowed due to the presence of the azepine ring.

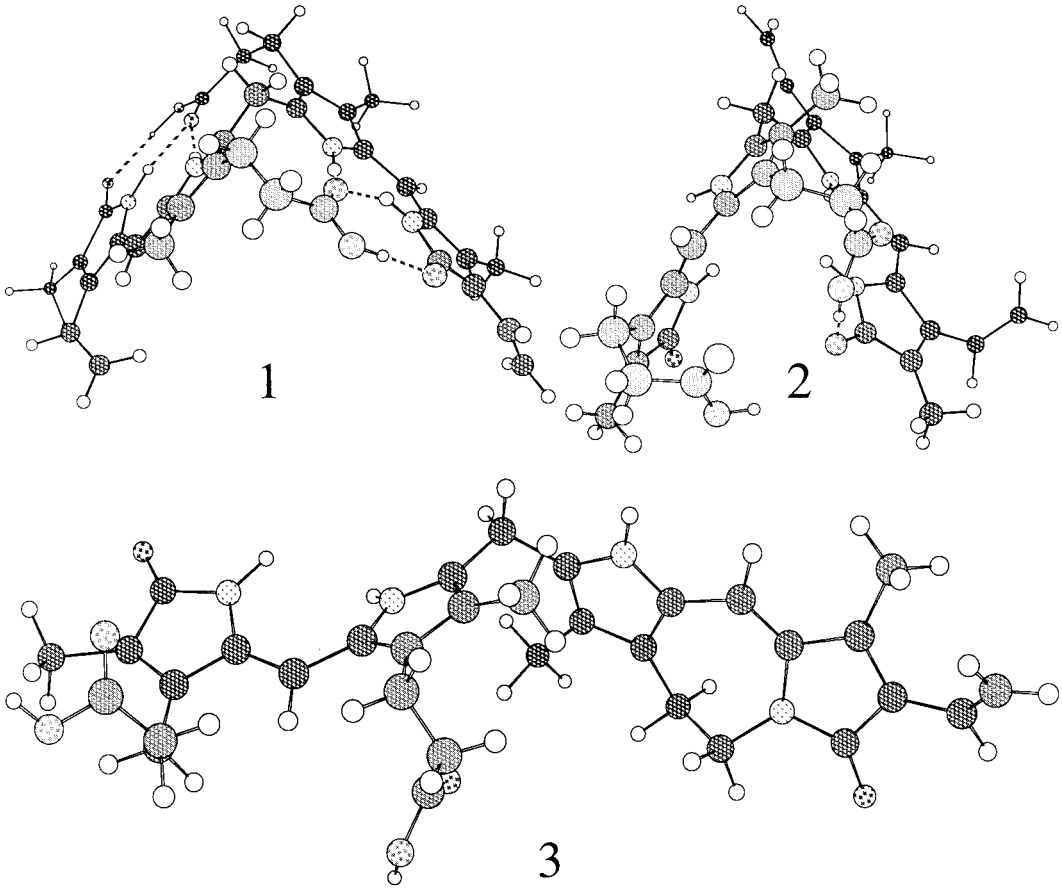

Figure 2. Ball and stick conformational representation of average conformers found for compounds **1–3** obtained after the MC/SD simulations. Dashed lines represent hydrogen bonds. The distances between the centroids of the pyrrinone rings are the following: 8.97 (**1**); 6.02 (**2**), 12.82 Å (**3**).

was observed for a monopropionic analogue substituted at C_7 studied before (compound **6**, ref 15). Unlike **2**, none of the above described hydrogen bonds were observed for compound **3**, where only a minor extent of interpropionic hydrogen bonding appears to take place.

Results from an independent calculation run following the MC(JBW)/SD protocol confirm the values of hydrogen bond distances and angles reported in Table 3 (results not shown).

Discussion

The position of the propionic acid chains and the availability of NHs and lactamic carbonyl groups for hydrogen bonding determines both the biological and physicochemical properties of bilirubins

The conformation of bilirubins, and in particular, the possibility of establishing intramolecular hydrogen bonds become critical factors which determine the need for glucuronidation to allow effective excretion of these compounds into the bile. Modification of the position of the carboxylic group across the tetrapyrrole system and blockage by alkylation of selected nitrogen positions influence molecular lipophilicity, a property which is generally attributed to the presence of intramolecular hydrogen bonding [ref 13 and references cited therein[15,30]].

In agreement with these notions, we observed a clear-cut difference in the conjugation behavior of two different isomers (**2** and **3**) of bilirubin IXα (**1**) with respect to the reference compound. Unlike bilirubin IXα (**1**), the natural positional isomer bilirubin IXδ (**2**) and the synthetically cyclized neobilirubin IXβ (**3**) are excreted in bile without being conjugated with glucuronic acid (Fig. 1). Similarly, Blanckaert et al.[12] found that bilirubin **2** is excreted mostly as its unconjugated form (84%). Our results are consistent with the more hydrophilic character observed for both compounds, as evidenced by their TLC behavior. The physicochemical properties of these isomers might play a critical role for the recognition by the UDP-sugar transferase.

The position of the maximum in UV–vis spectra informs about the general shape of the tetrapyrrolic system, since this parameter reflects the relative orientation of the transition dipoles of the dipyrrinone moieties.[13] The UV–vis spectrum in methanol or chloroform of compound **2** shows a band with an absorption maximum at 394 nm, which closely resembles the values observed for mesobilirubin IVα[31] and for a monopropionic analogue of bilirubin, both substituted at C_7 (compound **6**, Fig. 1 in ref 15). This fact is consistent with a closely folded

Table 3. Relative tendency to form hydrogen bonds for compounds **1**, **2** and **3**

Hydrogen bond	Compound **1**	Hydrogen bond	Compound **2**	Compound **3**
CO_8^3...$H_{23}N$		**CO_7^3...$H_{23}N$**		
Distance (Å)[a]	1.8 (0.20)	Distance (Å)[a]	2.7 (0.45)	> 3.0
N−H...O angle (°)[a]	160 (17.5)	N−H...O angle (°)[a]	165 (25)	n.d.
H...O=C angle (°)[a]	160 (15)	H...O=C angle (°)[a]	150 (20)	n.d.
%av (%−,%+)[b]	97 (90, 98)	%av (%−,%+)[b]	10 (2, 25)	1 (0, 2)
CO_8^3...$H_{24}N$		**CO_7^3...$H_{24}N$**		
Distance (Å)[a]	1.8 (0.20)	Distance (Å)[a]	2.0 (0.30)	
N−H...O angle (°)[a]	145 (15)	N−H...O angle (°)[a]	130 (20)	
H...O=C angle (°)[a]	130 (15)	H...O=C angle (°)[a]	140 (15)	
%av (%−,%+)[b]	89 (55, 97)	%av (%−,%+)[b]	51 (34, 61)	
OH_8^5...$O_{19}C$		**OH_7^5...$O_{19}C$**		
Distance (Å)[a]	1.8 (0.20)	Distance (Å)[a]	1.7 (0.15)	> 3.0
O−H...O angle (°)[a]	165 (12.5)	O−H...O angle (°)[a]	130 (12.5)	n.d.
H...O=C angle (°)[a]	120 (15)	H...O=C angle (°)[a]	135 (15)	n.d.
%av (%−,%+)[b]	95 (88, 97)	%av (%−,%+)[b]	80 (74, 82)	0 (0, 0)
CO_{12}^3...$H_{22}N$		**CO_3^3...$H_{23}N$**		
Distance (Å)[a]	1.8 (0.20)	Distance (Å)[a]	> 3.0	> 3,0
N−H...O angle (°)[a]	160 (15)	N−H...O angle (°)[a]	n.d.	n.d.
H...O=C angle (°)[a]	160 (15)	H...O=C angle (°)[a]	n.d.	n.d.
%av (%−,%+)[b]	96 (90, 98)	%av (%−,%+)[b]	0 (0; 0)	0 (0, 0)
CO_{12}^3...$H_{21}N$		**CO_3^3...$H_{24}N$**		
Distance (Å)[a]	1.8 (0.20)	Distance (Å)[a]	> 3.0	
N−H...O angle (°)[a]	145 (15)	N−H...O angle (°)[a]	n.d.	
H...O=C angle (°)[a]	150 (20)	H...O=C angle (°)[a]	n.d.	
%av (%−,%+)[b]	89 (54, 97)	%av (%−,%+)[b]	0 (0, 0)	
OH_{12}^5...O_1C		**OH_3^5...$O_{19}C$**		
Distance (Å)[a]	1.8 (0.20)	Distance (Å)[a]	> 3.0	> 3.0
O−H...O angle (°)[a]	165 (15)	O−H...O angle (°)[a]	n.d.	n.d.
H...O=C angle (°)[a]	120 (10)	H...O=C angle (°)[a]	n.d.	n.d.
%av (%−,%+)[b]	90 (87, 98)	%av (%−,%+)[b]	36 (35, 37)	0 (0, 0)
CO_8^3...H_{12}^5O		**CO_3^3...H_7^5O**		
Distance (Å)[a]	> 3.0	Distance (Å)[a]	> 3.0	1.95 (0.20)
O−H...O angle (°)[a]	n.d.	O−H...O angle (°)[a]	n.d.	145 (30)
H...O=C angle (°)[a]	n.d.	H...O=C angle (°)[a]	n.d.	120 (25)
%av (%−,%+)[b]	0 (0, 0)	%av (%−,%+)[b]	9 (6, 11)	35 (18, 40)
CO_{12}^3...H_8^5O		**CO_7^3...H_3^5O**		
Distance (Å)[a]	> 3.0	Distance (Å)[a]	> 3.0	1.85 (0.20)
O−H...O angle (°)[a]	n.d.	O−H...O angle (°)[a]	n.d.	125 (20)
H...O=C angle (°)[a]	n.d.	H...O=C angle (°)[a]	n.d.	145 (30)
%av (%−,%+)[b]	0 (0, 0)	%av (%−,%+)[b]	6 (5, 10)	38 (19, 45)

MC/SD simulations at 300 K in chloroform employing the AMBER* force field were run for 6 ns. This time allows the calculation to converge according to the criteria mentioned in Experimental. Four hundred thousand conformers were sampled for each isomer.

[a]The convention for bond distances and angles was stated in the legend to Table 1. These values correspond to the most populated states (mode), the half width of the distribution bell at half height is reported between parentheses.

[b]Population of H-bonded conformations, as estimated on each conformer found along the run. By definition, the H-bond X−H...Y−Z should meet the following criteria: average values (%av) were calculated for a H...Y distance < 2.5 Å, X−H...Y angle > 120° and H...Y−Z angle > 90°; %+ values result from a less stringent definition of the H-bond, namely, an H...Y distance < 2.75 Å, X−H...Y angle > 108° and H...Y−Z angle > 81°; %− values result from a more stringent definition, namely, an H...Y distance < 2.25 Å, X−H...Y angle > 132° and H...Y−Z angle > 99°.

conformation for compound **2**, where the dipyrrinone chromophores are oriented with nearly parallel transition dipoles.

At variance with this, the spectrum of bilirubin **3** is red-shifted, exhibiting a maximum at 433 nm. Two relevant structural features distinguish compound **3** from compound **2**: (i) a vinyl group is replaced by an ethyl substituent, and (ii) the double bond at C_{15}–C_{16} adopts the opposite configuration. In spite of these differences, the magnitude of the red-shift observed is such that it could only be reasonably explained by a generally more extended conformation for **3**. By comparison, compound **1**, which adopts predominantly a 'ridge tile' conformation, and presents two vinyl substituents, exhibits an absorption maximum at approx. 450 nm.[32]

In bilirubins, the ^{1}H NMR chemical shifts of pyrrolic and lactamic NHs provide a useful way of determining whether the dipyrrinone moieties participate in intramolecular hydrogen bonding. The pattern of these signals observed for compound **2** dissolved in chloroform, i.e. the pyrrolic NHs at δ 10.62 and 10.19 ppm, and the lactamic NHs at 9.35 and 9.21, agrees well with those found for two monopropionic analogues similarly substituted at C_7 (compound **6** in ref 15 and compound **2** in ref 31). By contrast, in bilirubin IXα, which establishes six intramolecular hydrogen bonds, the lactamic NHs

are shifted downfield (approx. 10.70 ppm) whereas the pyrrolic NHs are shifted upfield (approx. 9.30 ppm).[31] Taken together, these evidences indicate that an impairment exists in compound **2** for establishing hydrogen bonds. In addition, the high values for the chemical shifts observed for signals assigned to the acidic OHs in compound **2** (δ 14.35 and 13.24 ppm) suggest the involvement of the propionic side chains in hydrogen bonding, possibly to the opposite dipyrrinone. By comparison, a value of 12 ppm was observed for compounds where this OH does not participate in intramolecular H-bonding.[30]

In order to explain these data, conformational differences should account for the different tendency observed among these compounds to establish an intramolecular hydrogen bond network. Results from molecular modeling presented in this paper support this notion.

Molecular modeling reveals a folded conformation for bilirubin IXδ and an extended shape for neobilirubin IXβ

After a Monte Carlo conformational search and energy minimization, the most likely structures for compounds **2** and **3** were found. While the former adopts a closely folded structure, the latter exhibits conformational heterogeneity dominated by open and extended forms. This evident difference in overall shape brings about a distinct bias towards hydrogen bonding.

The analysis of the minimum energy conformers found for compound **2** reveals folded structures which exhibit alternative arrangements for intramolecular hydrogen bonding (Table 1). On average, each conformer exhibits 2–4 hydrogen bonds involving the carboxylates of side chains with the pyrrolic and lactamic NHs or the lactamic carbonyl group of the opposite dipyrrinone moiety. In fact, the propionic acid chain at C_7 plays a pivotal role, since its carboxylate group participates in a hydrogen bond network bridging the distal pyrrinone with the propionic side chain located at C_3. However, the presence of this substituent does not bear particular significance for the overall conformation of the molecule. In this regard, the global minimum conformer of a monopropionic analogue at C_7 (compound **6** in ref 15) does not differ much from $\mathbf{2_1}$ (RMS deviation less than 0.30 Å). Accordingly, the interplanar angle between the two dipyrrinone moieties is very similar.

A common feature of the other two conformers ($\mathbf{2_2}$ and $\mathbf{2_3}$) is the involvement of the propionic acid chain at C_3 in intramolecular hydrogen bonding with the carbonyl oxygen of the opposite pyrrinone (Table 1). Nevertheless, we anticipate that these conformers, although close in energy to the global minimum, would not be entropically favored due to the fact that a 20-member macrocycle should be established to form the $OH_3{}^5\ldots O_{19}C$ hydrogen bond. The ensuing MC/SD simulation (Table 3) substantiates this prediction.

A different picture emerges from the conformational analysis of compound **3**. None of the minimum energy conformers shows intramolecular hydrogen bonds linking the two dipyrrinone moieties. However, in all these structures, hydrogen bonds between propionic acid side chains appear.

For a given compound, an attempt to predict the relative proportions of hydrogen-bonded versus non-hydrogen bonded conformations based on their relative molecular mechanics energy according to a Boltzmann distribution will fail, because this neglects the entropy difference. In our case, where ring closure is an issue, this term can become significantly important. A calculation based on molecular mechanics energies alone would tend to overestimate the proportion of hydrogen bonded populations. By contrast, molecular dynamics could provide a better description of the conformational ensemble. We adopted an MC/SD method,[28] which had successfully predicted the hydrogen bonding pattern of a series of Gellman's diamides[33] and was later applied with benefit to estimate the different trend to establish a hydrogen bond network in two monopropionic analogues of bilirubin.[15]

This method, as applied to compound **2** (Table 3), showed that a severe impairment in the formation of the $CO_7{}^3\ldots H_{23}N$ and a lesser impediment for establishing the $CO_7{}^3\ldots H_{24}N$ bond indeed exist for compound **2**. However, given the semi-quantitative nature of this prediction, the existence of the latter is doubtful. By contrast, the $OH_7{}^5\ldots O_{19}C$ hydrogen bond is present (80%). This behavior is the same as that observed for an analogue of bilirubin similarly substituted with propionic acid at C_7 (compound **6** in ref 15). Accordingly, a close resemblance exists between the average structures predicted for these compounds. This bond appears to be a common feature present in folded structures (including 'ridge tile' and more closed structures).[15,31] The importance of this bond in stabilizing closed structures becomes specially clear after the finding of a close resemblance between conformer $\mathbf{2_3}$ and the average structure found for this compound. The C_7OOH/NH hydrogen bonds present in the former vanish in the latter, but both structures share the common $OH_7{}^5\ldots O_{19}C$ hydrogen bond. On the other hand, a minor participation in hydrogen bonding takes place between the propionic acid side chain at C_3 and the carbonyl group of the distal pyrromethenone. The folding observed for the average structure places the pyrrinone ends close in space (the distance between the centroids of these rings is 6.02 Å, Fig. 2), thus allowing the closure of the $OH_3{}^5\ldots O_{19}C$ hydrogen bond, which would otherwise be entropically unfavored. In addition, it is noteworthy that the interpropionic hydrogen bonds that appear in the minimized structures fail to show up in the average population. Taken together, these results point to the ancillary role played by the propionic acid substituent at C_3 as a factor influencing the global fold of the molecule.

For compound **3**, the absolute impediment in establishing hydrogen bonding with the distal pyrromethenone disallows folded structures. Expectedly, here again no $CO_7{}^3\ldots H_{23}N$ bond was observed. As a result, a minor extent of interpropionic hydrogen bonding appears to

take place, despite steric and entropic factors associated with the closure of the 14-member macrocycle where seven atoms should be almost coplanar and a concave face should exist at the central methine bridge.

In agreement with these predictions, the UV–vis evidence indicates that compound **2** indeed adopts a folded structure, whereas compound **3** should be more extended. In addition, the ^{1}H NMR data collected for compound **2** supports the notion that the pyrrolic and lactamic NHs should not be involved in hydrogen bonding. Compounds **2** and **3** share a similar polar character which differentiates both from bilirubin IXα (**1**). Accordingly, the prediction holds that, unlike **1**, which establishes an intramolecular hydrogen bond network with the participation of both propionic acid side chains, the carboxylic groups in **2** and **3** would be mostly free to interact with the solvent. The lack of an intramolecular hydrogen bond network does not necessarily imply the predominance of extended conformations. In particular, folded structures arise, even when an imperfect hydrogen bonding network occurs.

The proper simulation of the conformational ensemble through combined stochastic/molecular dynamics methods provides a realistic view of the average molecular shape from which to derive the behavior of these compounds. This is especially important for flexible molecules such as bilirubins, capable of establishing weak intramolecular interactions.

Experimental

Electronic absorption spectra were determined using a Hitachi U-2000 spectrophotometer. ^{1}H NMR spectra were recorded in deuterated chloroform on a Bruker MSL 300 spectrometer. Mass spectra were obtained with a TRIO 2-2000 spectrometer in the electronic ionization mode at 70 eV. Melting points were determined on a Kofler melting point apparatus and were not corrected. Microanalyses were performed using a Carlo Erba EA 1108 elemental analyzer. Bovine albumin (98–99%, w/w) was purchased from Sigma Chemical Co. All other chemicals used were of reagent grade. Solvents were distilled before use.

Synthesis of bile pigments

Bilirubin IXδ (2). Bilirubin IXδ (**2**, Scheme 1) used for ^{1}H NMR measurements was synthesized from the corresponding biliverdin (**4**) by reduction with sodium borohydride as described elsewhere.[15] Purification was carried out by TLC on silica gel plates (20×20 cm, silica gel F_{254}; 0.25 mm thick, Riedel de Haën), developed with chloroform:methanol:water (48:28:6, v/v). The yellow band containing the bilirubin pigment was scraped off and eluted from the silica with methanol. Evaporation under vacuum at room temperature afforded pure product.[20,21] The ^{1}H NMR spectra and H/D exchange experiments were carried out in a solution of 0.2 mg of compound **2** in 0.4 mL of deuterated chloroform, to which methanol-d_4 (100 μL) was added.

Neobiliverdin IXβ (5). The dimethyl ester of **5** (compound **7**) was prepared by total synthesis[22] and the product was saponified to the free acid **5** as follows. Biliverdin **7** (5 mg) was dissolved in a mixture of 5 mL tetrahydrofuran, 5 mL methanol and 10 mL of 2 M aqueous NaOH. This solution was kept in the dark under nitrogen at 37 °C during 3.5 h. The reaction mixture was then cooled, neutralized with glacial acetic acid and biliverdin **5** was extracted into chloroform, washed with water, dried over Na_2SO_4 and evaporated to dryness under vacuum at 35 °C. Crystallization from dichloromethane:hexane yielded green crystals, mp > 300 °C. The ^{1}H NMR spectrum taken in D_2O:NaOD shows the absence of OCH_3 groups, by comparison with the precursor. Anal. calcd[20] for $C_{33}H_{34}N_4O_6$ requires C, 68.04; H, 5.84; N, 9.62. Found: C, 68.18; H, 5.60; N, 9.80.

Biological experiments

Animals. Male Wistar rats weighing 300–400 g were obtained from the Animal House of Facultad de Farmacia y Bioquímica, Universidad de Buenos Aires.

Solution of pigments for injection. Compounds **4** and **5** (0.1 mg, 172 nmol) were dissolved in 0.05 mL of 0.1 M sodium hydroxide and 1 mL of albumin solution (10%, w/v, bovine albumin dissolved in 0.15 M NaCl solution) was added.[14]

Studies on biliary excretion

The rats were kept under anesthesia with diethylether and the common bile duct was cannulated with 10 cm of PE-10 tubing and protected from light with an aluminum foil. The left femoral vein was also cannulated (PE-10 tubing, 10 cm) and biliverdin solution was injected into the animal via the catheter for about 1 min with a 1 mL syringe. Immediately thereafter, a continous infusion (1 mL/h) of 0.15 M NaCl solution containing 5% (w/v) glucose was started and maintained for the length of the experiment.[14,34]

Throughout the experimental period, room temperature was 20 °C and the body temperature of rats was maintained with infrared lamps. The bile was collected in tubes placed on ice, protected from light and the volume (0.35 ± 0.04 mL per time point) was measured during the common bile duct cannulation (t = 0 min) and at 30, 60, 90, 120 and 150 min after injection. These values were corrected for the time taken by bile to flow through the dead volume of the cannula (19 μL).

Extraction from bile and separation of pigments

Biliary excretion of each pigment was studied on four Wistar rats. Bile samples were acidified by the addition of 8 vol. of glycine–HCl buffer (pH 1.8) followed by the addition of 2 vol. of ascorbic acid solution (100 mg/mL) saturated with NaCl.[35] An excess of salt was added to keep the solution saturated. The solution was then extracted several times at 0–4°C with chloroform:ethanol (1:1, v/v).[10,14,15,36] The concentrated extract from

each animal was then applied to silica gel plates (20×20 cm, silica gel F_{254}, 0.25 mm thick, Riedel de Haën), developed with chloroform:methanol:water (48:28:6, v/v). The plates were then dried and the yellow bands of bilirubins and the green bands of biliverdins were scraped off and eluted from the silica with methanol. The yellow bands of **1** and its conjugates were also scraped off and eluted from the silica with methanol: water (1:1, v/v). The amount of pigments **2** and **4** present in the eluates was estimated by measuring the absorbance in the range 390–430 nm ($\varepsilon = 46{,}000$) for the former and the ratio of absorbances at 372 ($\varepsilon = 47{,}000$) and 655 nm ($\varepsilon = 15{,}500$) for the latter.[21] Similarly, the amount of **3** and **5** was determined from the measurement of the absorbance at 433 nm ($\varepsilon = 40{,}700$) and the ratio of absorbances at 377 ($\varepsilon = 42{,}000$) and 633 nm ($\varepsilon = 35{,}600$), respectively. Finally, endogenous free bilirubin **1** and its conjugates were estimated by measuring the absorbance in the range 444–453 nm ($\varepsilon = 60{,}000$).[32]

Identification of bile pigments

Solutions of free and conjugated bilirubins were evaporated under vacuum at room temperature. Bilirubin **2** was compared with a reference compound by TLC on silica gel plates, as described before. Bilirubin **3** in methanolic solution spontaneously oxidizes to biliverdin **5** during evaporation of the solvent under reduced pressure. Therefore, the resulting biliverdin **5** was compared with a reference compound by TLC, as described above, and identified by mass spectrometry as its methyl ester **7**.[10]

The structures of compounds **2** and **1**, and the monoglucuronide and diglucuronide of **1** were confirmed by transformation into their corresponding azopigments. Methanolysis of these azopigments was followed by analysis of their methyl esters and conjugated sugars by established procedures.[6,10,14,35,36]

Conformational search

Molecular mechanics calculations were carried out with MacroModel 4.5/5.5 and BatchMin 4.5/5.5 [23] running on a SGI XS24Z workstation (R4000, 128 MB RAM, 19 GB hard disk) under the Irix 5.3 operating system or on a SGI O2 workstation (R10000, 320 MB RAM, 4 GB hard disk) under the Irix 6.3 operating system. The semiempirical method AM1 was implemented in HyperChem 3.0 [24] running on a PC (Pentium, 32 MB RAM, 1 GB hard disk) under Windows '95.

Optimized Monte Carlo search, energy minimization and relative stability of isomers

In this paper we used MM2* and AMBER* force fields (the versions of MM2 and AMBER, respectively, implemented in MacroModel[37]). By default, atomic partial charges are calculated from data in the molecular mechanics force field chosen. Both force fields use distance dependent dielectric electrostatics. The electrostatic equation used by MM2* uses partial charges and Coulomb's law, instead of the standard dipole–dipole electrostatics. MM2* includes approximate parameters for hydrogen bonds which were adjusted to mimic AMBER hydrogen bonding potentials. AMBER* is identical to authentic AMBER,[38] with additions. A number of generalized parameters have been added to the field to allow qualitative modeling on many types of molecules. The field is supplied with the united-atom AMBER charge set, and Kollman's 6,12-Lennard Jones hydrogen bonding treatment.[39]

The conformational search of bilirubins was carried out with an optimized Monte Carlo method[40] which employed the MM2* and AMBER* force fields, as implemented in MacroModel 4.5. Energy minimization used a conjugated gradient method, with a final gradient of 0.01 kcal/Å mol as the criterion for convergence. After the Monte Carlo steps, initial conformers were partially minimized (250 iterations), and the subset of resulting structures was further minimized until convergence. In this process, duplicate and high-energy structures were discarded. In the end, all non-enatiomeric conformers within a 5 kcal/mol window above the global minimum were tabulated. Atoms belonging to the tetrapyrrole backbone and the carbon atoms of the propionic acid substituents were taken into account for comparisons.

A protocol was employed for the conformational search of bilirubins **1**, **2** and **3** similar to that used before.[15] We started from structures with the following values for the central pair of dihedral angles (Φ_1, Φ_2): 0,0; 180,180; 0,180 and 180,0°. Ten rotational degrees of freedom, namely, Φ_1 through Φ_{10} (see Scheme 2) were considered. In all cases, between 70,000 and 100,000 Monte Carlo steps sufficed to sample the conformational ensemble.

The output conformers from the previous analysis were later optimized by the semiempirical method AM1. The protocol included a conjugated gradient method to approach the minimum and a final gradient threshold of 0.1 kcal/Å mol. A single point energy calculation on the optimized structures provided the values for the heats of formation.

Mixed Monte Carlo/stochastic dynamics

In order to simulate the conformational ensemble of the dipropionic bilirubins **1**, **2** and **3**, we applied a mixed Monte Carlo/stochastic dynamics (MC/SD) method,[28] which we tested before with monopropionic analogues of bilirubins.[15] In the course of the simulation, every SD time step is followed by an MC step. In all cases the total time was 6 ns after an initial equilibration time of 50 ps. A time step of 1.5 fs was used for the SD part.

Four hundred thousand conformers were sampled for each compound, resulting from an MC/SD simulation run at 300 K in chloroform, employing the semi-analytical solvation treatment GB/SA[41] and the AMBER* force field parameters. The default cut-off distance of 12 Å was increased to 50 Å in the electrostatics term. Ten degrees of freedom, namely, Φ_1 to Φ_{10}

(see Scheme 2) were also considered for this calculation. No constraint was put to torsions, and not more than two dihedral angles were allowed to change at each Monte Carlo step.

For each compound analysed, an independent simulation of the conformational ensemble following the Monte Carlo (jumping between wells)/stochastic dynamics protocol implemented in BatchMin 5.5[42] was carried out on the same set of torsion angles. Starting structures for these runs were taken from the output of each Monte Carlo conformational search.

A hydrogen bond is formed whenever (i) the distance between acceptor and donor is smaller than 2.5 Å, (ii) the angles N−H...O(=C) and (CO)O−H...O(=C) are greater than 120°, and (iii) the angles (N−)H...O=C and CO(O−) H...O=C are greater than 90°. Depending on the stringency of the criterion used for the definition of the hydrogen bond (see legend to Table 3), the actual calculated percentages vary within narrow limits.

Acknowledgements

This work was supported by grants from the National Research Council of Argentina (CONICET), the University of Buenos Aires, Fundación Antorchas and the European Union. M.E.M. is a recipient of a graduate student fellowship from CONICET. We thank the expert technical assistance with animal handling of Mr. Alejandro V. Ceccarelli and Ms. Cecilia Ricciardelli.

References

1. Heirwegh, K. P. M.; Blanckaert, N.; Compernolle, F.; Zaman, Z. *Biochem. Soc. Trans.* **1977**, *5*, 316.
2. Blanckaert, N.; Gollan, J.; Schmid, R. *Proc. Natl. Acad. Sci. USA* **1979**, *76*, 2037.
3. Brown, S. B. *Biochem. J.* **1976**, *159*, 23.
4. Billing, B. H.; Cole, P. G.; Lathe, G. H. *Biochem. J.* **1957**, *65*, 774.
5. O'Carra, P. In *Porphyrins and Metalloporphyrins*; Smith, K. M., Ed.; Amsterdam: Elsevier, 1975; pp 123–153.
6. Blumenthal, S. G.; Taggart, D. B.; Ikeda, R. M.; Ruebner, B. H.; Bergstrom, D. E. *Biochem. J.* **1977**, *167*, 535.
7. Heirwegh, K. P. M.; van Hees, G. P.; Leroy, P.; Van Roy, F. P.; Jansen, F. H. *Biochem. J.* **1970**, *120*, 877.
8. Gordon, E. R.; Chan, T. H.; Samodai, K.; Goresky, C. A. *Biochem. J.* **1977**, *167*, 1.
9. Yamaguchi, T.; Nakajima, H. *Eur. J. Biochem.* **1995**, *233*, 467.
10. Awruch, J.; Mora, M. E.; Lemberg, A.; Coll, C. T.; Frydman, R. B. *Biol. Chem. Hoppe-Seyler* **1994**, *375*, 617.
11. Blanckaert, N.; Heirwegh, K. P. M.; Compernolle, F. *Biochem. J.* **1976**, *155*, 405.
12. Blanckaert, N.; Heirwegh, K. P.M.; Zaman, Z. *Biochem. J.* **1977**, *164*, 229.
13. Person, R. V.; Peterson, B. R.; Lightner, D. A. *J. Am. Chem. Soc.* **1994**, 116, 42 and references cited therein.
14. Mora, M. E.; Bari, S. E.; Awruch, J. *Bioorg. Med. Chem. Lett.* **1997**, *7*, 1249.
15. Kogan, M. J.; Mora, M. E.; Awruch, J.; Delfino, J. M. *Bioorg. Med. Chem.* **1998**, *6*, 151.
16. Frydman, R. B.; Awruch, J.; Tomaro, M. L.; Frydman, B. *Biochem. Biophys. Res. Commun.* **1979**, *87*, 928.
17. Frydman, R. B.; Bari, S. E.; Tomaro, M. L.; Frydman, B. *Biochem. Biophys. Res. Commun.* **1990**, *171*, 465.
18. Bonnett, R.; Mc Donagh, A. F. *J. Chem. Soc. Perkin Trans. 1* **1973**, 881.
19. Tomaro, M. L.; Frydman, R. B.; Awruch, J.; Valasinas, A.; Frydman, B.; Pandey, R. K.; Smith, K. M. *Biochim. Biophys. Acta* **1984**, *791*, 350.
20. Heirwegh, K. P. M.; Fevery, J.; Blanckaert, N. *J. Chromatogr. Biomed. Applic.* **1989**, *496*, 1.
21. Heirwegh, K. P. M.; Blanckaert, N.; van Hess, G. *Anal. Biochem.* **1991**, *195*, 273.
22. Iturraspe, J.; Bari, S. E.; Frydman, B. *Tetrahedron* **1995**, *51*, 2243.
23. Mohamadi, F.; Richards, N. G. J.; Guida, W. C.; Liskamp, R.; Lipton, M.; Caufield, C.; Chang, G.; Hendrickson, T.; Still, W. C. *J. Comp. Chem.* **1990**, *11*, 440.
24. HyperChem for Windows, developed by and licensed from Hypercube Inc., Autodesk, Inc., 1992.
25. Bonnett, R.; Davies, J. E.; Hursthouse, N. B.; Sheldrick, G. M. *Proc. R. Soc. London, Ser. B.* **1978**, *202*, 249.
26. LeBas, G.; Allegret, A.; Mauguen, Y.; DeRango, C.; Bailly, M. *Acta Crystallogr., Sect. B* **1980**, *B36*, 3007.
27. A value of approx. 3 kcal/mol is estimated for a single hydrogen bond of this kind in bilirubins (see Boiadjiev, S. E.; Person, R. V.; Puzicha, G.; Knobler, C.; Maverick, E.; Trueblood, K. N.; Lightner, D. A. *J. Am. Chem. Soc.* **1992**, *114*, 10123).
28. Guarnieri, F.; Still, W. C. *J. Comp. Chem.* **1994**, *15*, 1302.
29. Senderowitz, H.; Guarnieri, F.; Still, W. C. *J. Am. Chem. Soc.* **1995**, *117*, 8211.
30. Hwang, K.; Timothy, A. D.; Lightner, D. A. *Tetrahedron* **1994**, *50*, 9919.
31. Holmes, D. L.; Lightner, D. A. *J. Heterocyclic Chem.* **1995**, *32*, 113 and references cited therein.
32. Crawford, J. M.; Ransil, B. J.; Potter, C. S.; Westmoreland, S. V.; Gollan, J. L. *J. Clin. Invest.* **1987**, *79*, 1172.
33. McDonald, D. Q.; Still, W. C. *J. Am. Chem. Soc.* **1994**, *116*, 11550.
34. Sieg, A.; Stiehl, A.; Heirwegh, K. P. M.; Fevery, J.; Raedsch, R.; Kommerell, B. *Hepatology* **1989**, *10*, 14.
35. Blanckaert, N.; Fevery, J.; Heirwegh, K. P. M.; Compernolle, F. *Biochem. J.* **1977**, *164*, 237.
36. Awruch, J.; Lemberg, A.; Frydman, R. B.; Frydman, B. *Biochim. Biophys. Acta* **1982**, *714*, 209.
37. MacroModel, A Primer, Version 4.5, Department of Chemistry, Columbia University, New York, NY 10027, 1994.
38. Weiner, S. J.; Kollman, P. A.; Case, D. A.; Singh, U. C.; Ghio, C.; Alagona, G.; Profeta, Jr. S.; Weiner, P. *J. Am. Chem. Soc.* **1984**, *106*, 765.
39. Ferguson, D. M.; Kollman, P. A. *J. Comp. Chem.* **1990**, *12*, 620.
40. Chang, G.; Guida, W. C.; Still, W. C. *J. Am. Chem. Soc.* **1989**, *111*, 4379.
41. Still, W. C.; Tempczyk, A.; Hawley, R. C.; Hendrickson, T. *J. Am. Chem. Soc.* **1990**, *112*, 6127.
42. MacroModel, A Primer, Version 5.5, Department of Chemistry, Columbia University, New York, NY 10027, 1996, 125.